Journal of Chromatography, 509 (1990) 287–299
Elsevier Science Publishers B.V., Amsterdam

CHROM. 22 207

Computer-assisted choice of electrolyte systems and spacing constituents for two-dimensional capillary isotachophoresis

J. MARÁK
Institute of Radioecology and Applied Nuclear Techniques, Chrapčiakova 1, 052 01 Spišská Nová Ves (Czechoslovakia)
J. LAŠTINEC and D. KANIANSKY*
Institute of Chemistry, Faculty of Science, Komenský University, Mlynská Dolina CH-2, 842 15 Bratislava (Czechoslovakia)
and
V. MADAJOVÁ
Department of Analytical Chemistry, Faculty of Science, Komenský University, Mlynská Dolina CH-2, 842 15 Bratislava (Czechoslovakia)

ABSTRACT

Equations enabling interferences due to sample matrix constituents in two-dimensional isotachophoretic analysis using the spike method to be estimated were derived. A computer program and a procedure based on these equations were developed for searching for optimum and less time consuming electrolyte systems and spacing constituents. The procedure, intended mainly for the trace analysis of the constituents present in complex ionic matrices, was examined in experiments with benzoate as a trace analyte. A model mixture of 50 arbitrarily chosen anionically migrating UV light-absorbing constituents simulated the sample matrix. A reasonable agreement in ordering the electrolyte systems according to interfering contributions of the sample matrix was obtained between the experimental and calculated data. Some discrepancies found in the examination of the proposed procedure are discussed.

INTRODUCTION

Column-coupling capillary isotachophoresis (CC-ITP), as first described by Everaerts *et al.*[1], has several advantages in the analysis of complex ionic mixtures when both a high performance index of the separation compartment[2] and high resolution rates[3] are desired. In addition, this technique enables two-dimensional (2D) ITP separations to be performed when some general requirements concerning 2D separations in the column-coupling systems[4] are met. It can easily be deduced that for ITP they can be formulated in the following way: (i) the sample constituents are subjected to two largely independent separation steps, *i.e.*, the leading electrolytes in the coupled columns should be chosen among those characterized by low similarities[5];

0021-9673/90/$03.50

and (ii) the separation achieved in the first dimension is not nullified by the formation of mixed zones in the second separation step.

The latter requirement clearly implies that in CC-ITP maximum analytical benefit, *i.e.*, a true 2D separation, can be achieved when apart from the analyte only a minimum number of sample constituents are transferred from the first column for a final separation in the second column. It also suggests that a tandem arrangement of independently refillable columns[6] is, in general, inconvenient for 2D ITP separations.

In ITP, selective detectors often provide considerably lower detection limits than high-resolution universal detectors, especially when the spike[7–9] and/or steady-state mixed zone[10] methods are employed. Therefore, 2D ITP separations combined with the selective detection of the analytes by one of these methods appear promising for trace analytical work, potentially with no or at least minimized sample preparation. In such a combination, appropriate discrete spacing constituents added to the sample can be effective in achieving the following goals[11]: (i) a well defined transfer of the sample fraction of analytical interest from the first separation step for a final separation in the second separation step; and (ii) favourable detection conditions for the analyte in the second separation step.

From the practical point of view, a choice of the leading electrolytes and spacing constituents giving a minimum bias in the detection and/or determination of the analyte can be both time and labour consuming when performed only experimentally. When the qualitative sample composition is known, computer simulation provides a means of reducing this problem[12–14]. Unfortunately, in the analysis of trace constituents present in complex matrices the sample composition is known only seldom and, therefore, this straightforward approach has limited applicability in these instances.

The aim of this work was to elaborate a procedure that could facilitate a search for suitable combinations of the leading electrolytes and spacing constituents in 2D ITP when the analytical evaluation is performed by the spike method from the response of the selective detector. The procedure described here is based on relationships that allow a comparison of various electrolyte systems and discrete spacers via parameters characterizing (potential) interferences in the determination of the analyte due to matrix constituents. A computer program providing numerical values of these parameters was written. The proposed procedure was applied to the determination of benzoate present at a $5 \cdot 10^{-6}$ mol/l concentration in a mixture containing 50 anionic constituents representing the sample matrix.

THEORETICAL

Interfering constituents in 2D ITP analysis of complex mixtures

2D ITP separation with selective detection of the analyte in the second separation dimension (2nd D) is illustrated schematically in Fig. 1. From basic principles of ITP[15], it is clear that the migration configuration shown in Fig. 1 requires that in the first separation dimension (1st D) the following conditions are fulfilled:

$$ {}_1\bar{m}_{X,A} < {}_1\bar{m}_{A,A} \tag{1a}$$

and

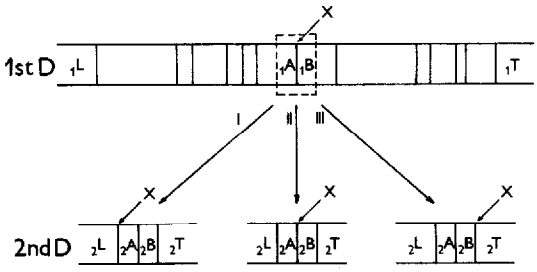

Fig. 1. Scheme of 2D ITP analysis in the column-coupling instrument with selective detection of the analyte migrating in the interzonal boundary layer between the zones of spacers A and B. The dashed box indicates that part of the sample fraction transferred for a final separation in the 2nd D. I, II, III = possible migration configuration of the analyte (X) under the working conditions employed in the 2nd D when the formation of mixed zones and/or a zone-electrophoretic migration of the analyte do not occur. L, T = leading and terminating constituents, respectively; 1, 2 = indices of the separation dimensions.

$$ {}_1\bar{m}_{X,B} > {}_1\bar{m}_{B,B} \tag{1b} $$

where the subscript 1 identifies the 1st D, the first subscripts on the right relate to the constituents and the second subscripts on the right identify the zones.

As we consider the complex ionic nature of the sample, it can be expected that the analyte in its migration position is accompanied by some of the sample constituents. In our particular case, under the conditions employed in the 1st D, matrix constituents (Z) will interfere, giving a response to the detector and meeting the conditions

$$ {}_1\bar{m}_{Z,A} \leqslant {}_1\bar{m}_{A,A} \tag{2a} $$

and

$$ {}_1\bar{m}_{Z,B} \geqslant {}_1\bar{m}_{B,B} \tag{2b} $$

where the sign of equality indicates that interferents present within the zones of the spacers are also included (the steady-state mixed zones). For the sake of simplicity we assume in this work that the interferents are strong and monovalent, weakly ionic constituents and that only acid–base equilibria are involved in the separation. Then for the effective mobilities of the interfering constituents we can write

$$ {}_1\bar{m}_{Z,i} = {}_1\alpha_{Z,i1}m_Z \tag{3} $$

where ${}_1\alpha_{Z,i}$ is a molar fraction (degree of dissociation) of the charged ionic form of a given constituent in the ith zone. The molar fraction and the corresponding dissociation constant (K_Z) are related via the Henderson–Hasselbach equation

$$ {}_1\alpha_{Z,i} = K_Z/({}_1[H]_i + K_Z) \tag{4} $$

where ${}_1[H]_i$ is the concentration of H^+ ions in the ith zone. Eqns. 3 and 4 enable the conditions (2a) and (2b) to be modified into the following form:

$$ {}_1m_Z \leqslant {}_1\bar{m}_{A,A}(1 + 10^{pK_Z - {}_1pH_A}) \tag{5a} $$

and

$$ {}_1m_Z \geqslant {}_1\bar{m}_{B,B}(1 + 10^{pK_Z - {}_1pH_B}) \tag{5b} $$

where ${}_1pH_A$ and ${}_1pH_B$ are the pH values in the zones of spacers in the 1st D.

The ionic mobilities and pK values of both the analyte and spacing constituents and the composition of the leading electrolyte used in the 2nd D determine the actual migration configuration in this separation step. When neither zone electrophoretic migration of the analyte nor formation of a mixed zone of the analyte with one of the constituents occurs, then in this instance one of the migration configurations shown in Fig. 1 will be achieved in the 2nd D. For the interfering constituents analogous relationships to those for the 1st D are valid. Hence, for the configuration discussed further (III in Fig. 1), we can write the conditions

$$ {}_2m_Z \leqslant {}_2\bar{m}_{B,B}(1 + 10^{pK_Z - {}_2pH_B}) \tag{6a} $$

and

$$ {}_2m_Z \geqslant {}_2\bar{m}_{T,T}(1 + 10^{pK_Z - {}_2pH_T}) \tag{6b} $$

where the subscript 2 identifies the 2nd D.

Clean-up efficiency in 2D ITP

Characteristic parameters for ITP migrating zones can be calculated, *e.g.*, as elaborated by Beckers and co-workers[15,16]. The data obtained permit the use of eqns. 5 and 6 to calculate plots defining regions of interfering constituents (in coordinates of ionic mobility *vs.* pK value) for both separation steps. When a uniform distribution of the interfering constituents within given ranges of ionic mobilities and pK values is assumed, then the areas of the regions of interferents can be interpreted in the following way (see also Fig. 2): the area ${}_1A$ is a measure of interfering matrix constituents unseparable from the analyte under the conditions employed in the 1st D (the area ${}_2A$ is an analogous measure for the 2nd D); an overlap of the areas ${}_1A$ and ${}_2A$ (${}_{1-2}A$ in Fig. 2) serves as a measure of the constituents unseparable from the analyte with a given combination of the leading electrolyte and spacing constituents; the unoverlapped part of the area ${}_1A$ corresponds to that part of interfering constituents which is separated from the analyte under the conditions employed in the 2nd D; and the unoverlapped part of the area ${}_2A$ represents that part of the constituents which interfere under the conditions employed in the 2nd D but which cannot be present in the sample fraction transferred into the 2nd D.

From this interpretation, it is apparent that the ratio ${}_{1-2}A/{}_1A$ is a measure of a clean-up efficiency of the 2nd D for a given sequence of the leading electrolytes and for the spacing constituents employed. As the clean-up efficiency of the 2nd D (ΔS_x) is zero when the same leading electrolytes and spacing constituents are used in both separation steps, it is reasonable to define this parameter via the equation

$$ \Delta S_x = 1 - {}_{1-2}A/{}_1A \tag{7} $$

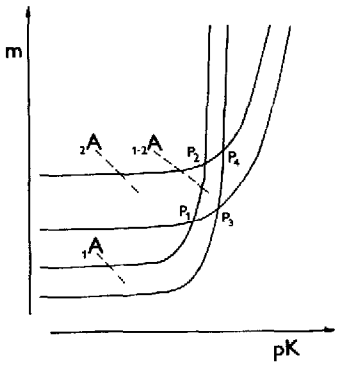

Fig. 2. Schematic illustration of plots defining regions of interfering constituents in the coordinates of ionic mobility (m) *vs.* pK value. ${}_1A$ = region (area) of interfering constituents accompanying the analyte in the 1st D (these constituents are transferred with the analyte for a final separation in the 2nd D). Solid lines defining this region correspond to the interfering constituents migrating in the zones of spacing constituents. ${}_2A$ = region (area) of interfering constituents accompanying the analyte under the working conditions employed in the 2nd D. Solid lines have an analogous meaning to those in the 1st D. ${}_{1-2}A$ = region (area) corresponding to the matrix constituents unseparable from the analyte in a given combination of the electrolyte systems employed in both dimensions. P_1–P_4 = points of intersection of the solid lines defining the regions ${}_1A$ and ${}_2A$.

Despite the above simplifying assumptions, eqn. 7 may serve as a realistic estimate of the clean-up efficiency of the 2nd D for matrices with characteristic "continuous" mobility profiles[17–19].

It is apparent that by using the same leading electrolyte in both columns with the same spacing constituents, ${}_{1-2}A = {}_1A = {}_2A$ and $\Delta S_x = 0$. The value $\Delta S_x = 1$, *i.e.*, a maximum clean-up efficiency in the 2nd D, is meaningless as it requires that ${}_{1-2}A = 0$. In other words, in this instance the areas ${}_1A$ and ${}_2A$ do not overlap and, therefore, the analyte cannot migrate in the desired position in the 2nd D. Hence only the values $\Delta S_x < 1$ have a practical meaning.

Comparison of various combinations of leading electrolytes and spacing constituents

In 2D ITP it is desirable to achieve a high clean-up efficiency in the 2nd D($\Delta S_x \rightarrow 1$). On the other hand, this need not to correspond to an optimum combination of the leading electrolytes and/or spacing constituents because it can be due to a high value of ${}_1A$ (a wide fraction transferred for a final separation in the 2nd D). Therefore, a comparison of various combinations of the electrolyte systems and spacing constituents is more convenient via their ${}_{1-2}A$ values since this parameter may serve as an absolute measure of interfering constituents unresolved from the analyte.

It is apparent that an optimum combination of the leading electrolytes and discrete spacers is characterized by a minimum value of ${}_{1-2}A$ (ideally, ${}_{1-2}A \rightarrow 0$). Once such a combination has been found, it is necessary to select an optimum sequence of the leading electrolytes in the separation steps. From general requirements (see Introduction) it can be seen that it is desirable to transfer a minimum of the matrix constituents from the first column for a final separation in the second column. This is fulfilled when the leading electrolyte with associated spacers having a lower area defining the interfering constituents is used in the first column. Moreover, such

a criterion is favourable when we consider also the volumes of the columns advantageously used in CC-ITP[1,20].

Equations for calculations of parameters for pre-experimental choice of leading electrolytes and spacing constituents

Eqns. 5 and 6 enable one to calculate and plot interfering constituents as shown in Fig. 2. Numerical values of the areas ${}_{1-2}A$, ${}_1A$ and ${}_2A$, important for the choice of optimum working conditions, can be obtained by solving the following integrals within reasonable chosen limits of pK values (0–11 in this instance) and within limits defined by the pK values corresponding to the points of intersection ($P_1 - P_4$ in Fig. 2):

$$ {}_1A = \int_0^{11} ({}_1\bar{m}_{A,A} \cdot 10^{pK_Z - {}_1pH_A} + {}_1\bar{m}_{A,A})\, dpK_Z - \int_0^{11} ({}_1\bar{m}_{B,B} \cdot 10^{pK_Z - {}_1pH_B} + {}_1\bar{m}_{B,B})\, dpK_Z \quad (8) $$

$$ {}_2A = \int_0^{11} ({}_2\bar{m}_{B,B} \cdot 10^{pK_Z - {}_2pH_B} + {}_2\bar{m}_{B,B})\, dpK_Z - \int_0^{11} ({}_2\bar{m}_{T,T} \cdot 10^{pK_Z - {}_2pH_T} + {}_2\bar{m}_{T,T})\, dpK_Z \quad (9) $$

$$ \begin{aligned} {}_{1-2}A = {} & \int_{pK'_{Z_1}}^{pK'_{Z_2}} ({}_1\bar{m}_{A,A} \cdot 10^{pK_Z - {}_1pH_A} + {}_1\bar{m}_{A,A})\, dpK_Z - \int_{pK'_{Z_1}}^{pK'_{Z_2}} ({}_2\bar{m}_{T,T} \cdot 10^{pK_Z - {}_2pH_T} + {}_2\bar{m}_{T,T})\, dpK_Z + \\ & \int_{pK'_{Z_2}}^{pK'_{Z_3}} ({}_2\bar{m}_{B,B} \cdot 10^{pK_Z - {}_2pH_B} + {}_2\bar{m}_{B,B})\, dpK_Z - \int_{pK'_{Z_2}}^{pK'_{Z_3}} ({}_2\bar{m}_{T,T} \cdot 10^{pK_Z - {}_2pH_T} + {}_2\bar{m}_{T,T})\, dpK_Z + \\ & \int_{pK'_{3_1}}^{pK'_{Z_4}} ({}_1\bar{m}_{B,B} \cdot 10^{pK_Z - {}_1pH_B} + {}_1\bar{m}_{B,B})\, dpK_Z - \int_{pK'_{Z_3}}^{pK'_{Z_4}} ({}_2\bar{m}_{T,T} \cdot 10^{pK_Z - {}_2pH_T} + {}_2\bar{m}_{T,T})\, dpK_Z \end{aligned} \quad (10) $$

The solutions of the integrals[21] are illustrated for the first integral in eqn. 8

$$ {}_1\bar{m}_{A,A} \cdot 10^{-{}_1pH_A} \cdot \int 10^{pK_Z}\, dpK_Z + \int {}_1\bar{m}_{A,A}\, dpK_Z \quad (11) $$

where the solution is

$$ {}_1\bar{m}_{A,A}/(\ln 10) \cdot 10^{pK_Z - {}_1pH_A} + {}_1\bar{m}_{A,A} pK_Z + C \quad (12) $$

In the case in Fig. 2, for the points of intersection the following conditions are valid:

$$P_1: \quad {}_1\bar{m}_{A,A} \cdot 10^{pK'_{Z_1} - {}_1pH_A} + {}_1\bar{m}_{A,A} = {}_2\bar{m}_{T,T} \cdot 10^{pK'_{Z_1} - {}_2pH_T} + {}_2\bar{m}_{T,T} \tag{13}$$

$$P_2: \quad {}_1\bar{m}_{A,A} \cdot 10^{pK'_{Z_2} - {}_1pH_A} + {}_1\bar{m}_{A,A} = {}_2\bar{m}_{B,B} \cdot 10^{pK'_{Z_2} - {}_2pH_B} + {}_2\bar{m}_{B,B} \tag{14}$$

$$P_3: \quad {}_1\bar{m}_{B,B} \cdot 10^{pK'_{Z_3} - {}_1pH_B} + {}_1\bar{m}_{B,B} = {}_2\bar{m}_{T,T} \cdot 10^{pK'_{Z_3} - {}_2pH_T} + {}_2\bar{m}_{T,T} \tag{15}$$

$$P_4: \quad {}_1\bar{m}_{B,B} \cdot 10^{pK'_{Z_4} - {}_1pH_B} + {}_1\bar{m}_{B,B} = {}_2\bar{m}_{B,B} \cdot 10^{pK'_{Z_4} - {}_2pH_B} + {}_2\bar{m}_{B,B} \tag{16}$$

which provide pK values (pK'_{Z_1}–pK'_{Z_4}) required for the solutions of the integrals in eqn. 10.

EXPERIMENTAL

Instrumentation

A CS isotachophoretic analyser (VVZ PJT, Spišká Nová Ves, Czechoslovakia) was used in the column-coupling configuration of the separation unit. The analytical column of the analyser was provided with an on-column UVD1 photometric detector (VVZ PJT) and the detection wavelength was 254 nm. The signal from this detector was evaluated with an HP 3390A reporting integrator (Hewlett-Packard, Avondale, PA, U.S.A.). The program, written in T-Pascal 1.0 (VÚVT, Žilina, Czechoslovakia), runs on a DATAS-AT computer (DataSystem, Bratislava, Czechoslovakia).

Chemicals

Chemicals used for the preparation of the leading and terminating electrolytes were obtained from Sigma (St. Louis, MO, U.S.A.), Serva (Heidelberg, F.R.G.), Reanal (Budapest, Hungary) and Lachema (Brno, Czechoslovakia). They were purified by current methods[22]. Water supplied by a Rodem 1 demineralization unit (OPP, Tišnov, Czechoslovakia) and further purified on Amberlite MB-1 mixed-bed ion exchanger (BDH, Poole, U.K.) was used for the preparation of the solutions.

Hydroxyethylcellulose 4000 (Serva) was added to the leading electrolytes as an anticonvective additive. Its stock solutions were purified on Amberlite MB-1 mixed-bed ion exchanger.

RESULTS AND DISCUSSION

Description of the calculations

Calculations of the parameters required for a pre-experimental choice of the working conditions (see Theoretical) were carried out in the following steps: calculations of characteristic parameters of the zones of spacing constituents and the terminating zone in the ITP steady state were carried out with the program ITER[15,16], physico-chemical data published by Hirokawa *et al.*[23] serving as input data; calculations to examine whether the conditions (1) and/or analogous conditions for

the 2nd D are met; by using eqns. 5 and 6, boundaries determining the regions of interfering constituents were calculated (see also Fig. 2); the area of overlap ($_{1-2}A$) and the areas of the regions of interfering constituents ($_1A$ and $_2A$) were calculated from eqns. 8–10; calculations of the clean-up efficiency of the 2nd D with the aid of eqn. 7.

A detailed description of these calculations is apparent from the algorithm given in Fig. 3. In the calculations we assumed that the interfering constituents have ionic mobilities in the range $0–10^{-3}$ cm^2 V^{-1} s^{-1} while their pK values are 0–11. The results of the calculations and graphical plots analogous to those shown schematically in Fig. 2 could be displayed on a screen and/or printed.

Comparison of calculated and experimental data

In an experimental examination of the proposed procedure, benzoate was chosen as an analyte and a mixture of arbitrarily chosen UV light-absorbing constituents (Table I) migrating anionically under the working conditions studied

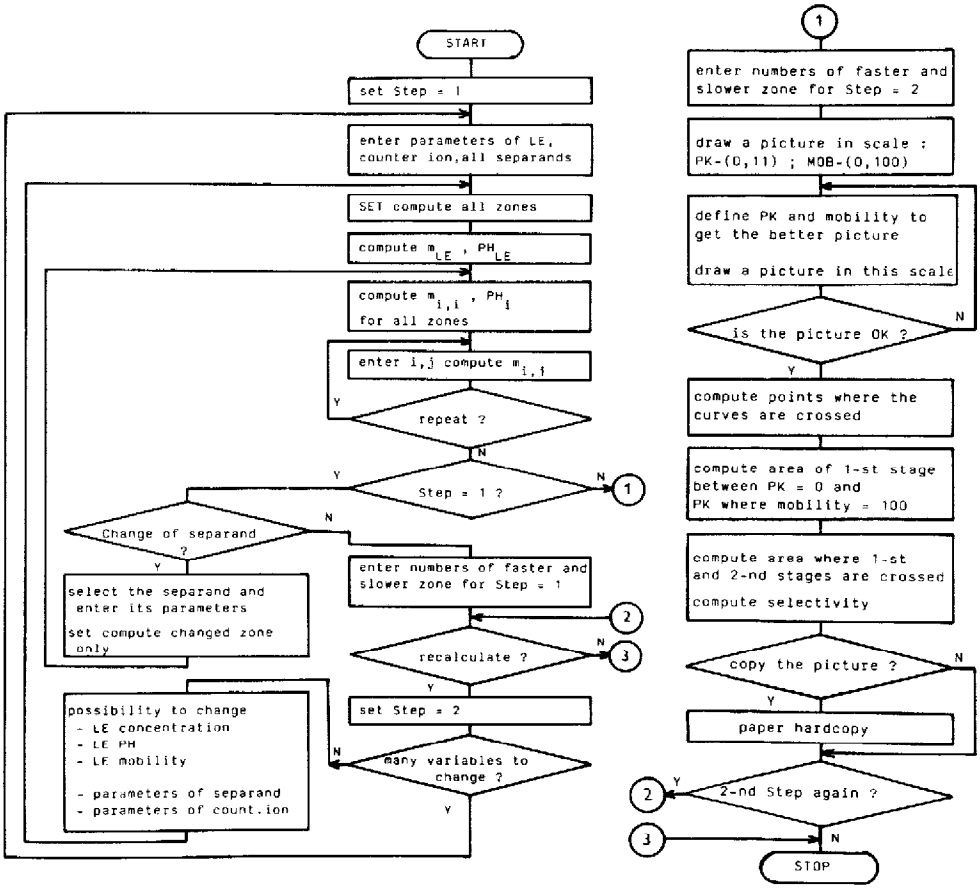

Fig. 3. Algorithm for the calculation of the steady-state parameters of the zones and the parameters characterizing the electrolyte systems and spacing constituents from the point of view of the interferences due to the sample matrix constituents.

TABLE I

COMPOSITION OF MODEL MIXTURE USED AS A SAMPLE MATRIX

Acetylsalicylic, anthranilic, *p*-aminobenzoic, *p*-amino-2-naphthol-4-sulphonic, anthraquinone-2-sulphonic, 2-amino-8-naphthol-3,6-disulphonic, *p*-aminosalicylic, 2-amino-5-naphthol-7-sulphonic chromotropic, cinnamic, 2-amino-5-naphthol-3,6-disulphonic, 4-chlorobenzoic, 2,4-dihydroxybenzoic, fumaric, 5,5-diethylbarbituric, 2,4-dinitrobenzoic, 3,5-dinitrosalicylic, furylacrylic, 3,5-dinitrobenzoic, 4,4′-diaminostilbene-2,2′-disulphonic, β-indolylacetic, 2,5-dichlorobenzenesulphonic, *m*-hydroxybenzoic, hippuric, 2,4,6-trimethylbenzenesulphonic, 2-ketoglutaric, mandelic, maleic, methanilic, *m*-nitrobenzoic, *p*-nitrobenzoic, 3-nitrophthalic, nicotinic, naphthylacetic, 2-naphthoxyacetic, 4-nitrophthalic, 3-nitrobenzenesulphonic, phenylanthranilic, picric, pyrogallolcarbonic, phenylphosphoric, phthalic, sulphosalicylic, sorbic, sulphanilic, salicylic, 2,4,6-trinitrobenzoic and *p*-toluenesulphonic acids, 2,6-dinitrophenol and 2,4-dinitrophenol

served as a sample matrix. The concentrations of the matrix constituents in the injected samples (valve injection with a 30-μl sample loop) were *ca.* 0.2 ppm to achieve a linear response of the photometric detector for the constituents present in the migration position of benzoate in all experiments.

The isotachopherograms in Fig. 4 provide detection profiles of the sample matrix in the operational systems in which the separations were performed, mainly according to pK values (pH 3.2) and according to ionic mobilities (pH 4.7). With respect to some inherent limitations of the separation unit employed (the same terminating constituents for both columns), these systems were taken as lower (pH 3.2) and upper (pH 4.7) pH limits in this work.

When the columns were filled with the same leading electrolytes ("single" column mode of analysis) and only that part of the sample containing the analyte with the adjacent parts of the zones of spacing constituents were transferred to the second column for detection, we obtained isotachopherograms (Fig. 5) that provided the following information: (i) the total amount of photometrically detectable impurities (measured in integrator counts) present in the migration position of benzoate and originating from the electrolyte system used (Fig. 5a); when desired this contribution to the systematic error in the quantification of the analyte could be subtracted as a blank value; (ii) the total amount of the matrix constituents present in the migration position of the analyte and detectable by the photometric detector [measured as in (i)]; its value (Fig. 5b) is related to the areas ${}_1A$ and/or ${}_2A$ as defined under Theoretical; (iii) the response of the detector corresponding to the analyte (the difference between the numbers of counts as measured in Fig. 5c and b); and (iv) characterization of the sample fraction transferred for a final separation in the second column when a given electrolyte system is used in the first column in 2D runs.

Isotachopherograms from the photometric detector shown in Fig. 6 were obtained under the conditions with given sequences of the leading electrolytes. The data provided by the detector (measured in the above way) were taken as experimental estimates of contributions of the electrolyte systems (Fig. 6a) and matrix constituents (the difference between Fig. 6b and a) to the quantification of the analyte. It is clear that the runs with the sample matrix (Fig. 6b) provided the experimental data corresponding to the areas ${}_{1-2}A$ (Fig. 2) calculated as described above.

The data obtained from the described experiments and those from the calculations are summarized in Table III. A direct comparison of the experimental and

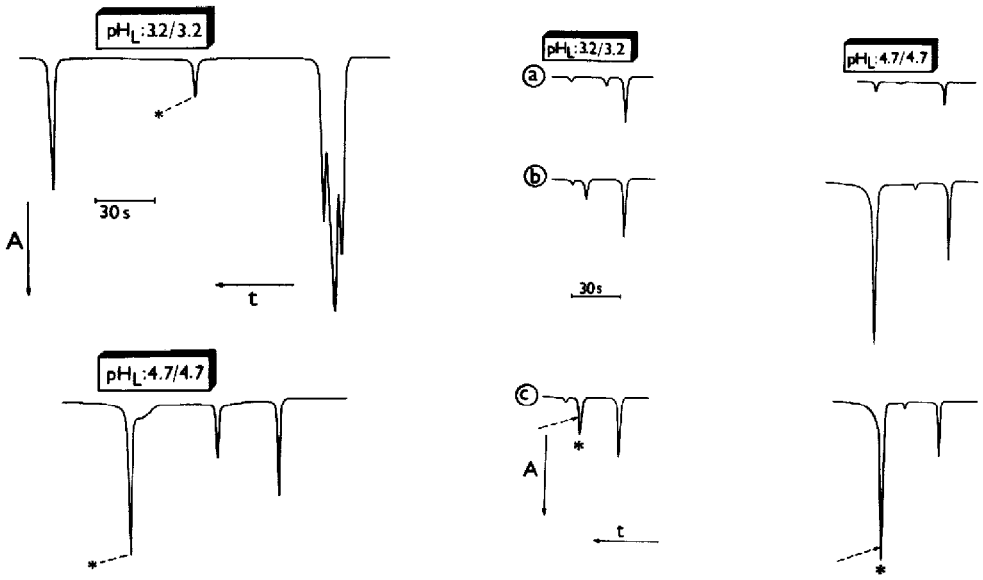

Fig. 4. Isotachopherograms from the analyses of a model mixture representing the sample matrix (see Table I and the text). Only the traces from the photometric detector in the second column are given. Asterisks mark the migration positions of benzoate. Succinate and glutarate served as the discrete spacers in these experiments. A,t = increasing light absorption and time, respectively. The driving currents were 200 and 45 μA in the first and second columns, respectively. The operational systems (Table II) are indicated via their pH_L values.

Fig. 5. Contributions of the interferences from (a) the electrolyte system and (b) the sample matrix to (c) the quantification of benzoate ($5 \cdot 10^{-6}$ mol/l concentration in the injected sample). Both columns were filled with identical leading electrolytes (see the corresponding data in this figure and Table II) and only that part of the sample containing the analyte and adjacent regions of the zones of spacers (succinate and glutarate) were transferred into the second column for detection. Arrows indicate peak heights corresponding to the interfering constituents in the migration position of benzoate (marked with asterisks). For the driving currents and the meaning of the remainder of the symbols, see Fig. 4. The operational systems (Table II) are indicated via their pH_L values.

calculated data of primary interest ($_{1-2}A$ and $_{1-2}A^*$ in Table III) was almost impossible as they were obtained in different physical units mutually convertible only with difficulty. Therefore, the practical utility of the choice of the electrolyte systems for 2D ITP via the calculations based on our simple model could be evaluated only qualitatively. As our main aim was to develop a procedure to simplify the search for optimum working conditions, this is an acceptable way. In the evaluation, the electrolyte systems considered in the investigation were ordered according to increasing $_{1-2}A$ values, *i.e.*, in the order of expected bias in the determination of the analyte. From the tabulated data the following order of the electrolyte systems was obtained: II < III < IV < I. It should be noted that the $_{1-2}A$ values for systems II and III are *a priori* identical (different sequences of the same pair of leading electrolytes). Therefore, $_1A$ values were decisive in their ordering (see Theoretical). The same electrolyte systems ordered on the basis of experimental data ($_{1-2}A^*$ values in Table III) gave the following order: II < III < I < IV. A comparison of the ordered

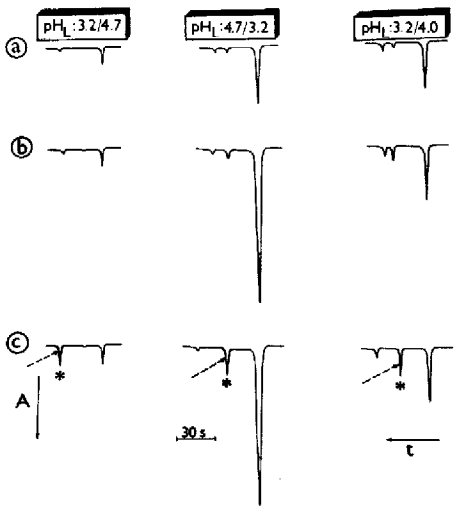

Fig. 6. Contributions of the interferences from (a) the electrolyte system and (b) the sample matrix to (c) the quantification of benzoate in the 2D mode of the ITP analysis for various sequences of the leading electrolytes (see the data in this figure and Table II). Arrows indicate peak heights corresponding to the interfering constituents migrating in the same position as benzoate (marked with asterisks) under given working conditions. The same samples as in Fig. 5 were injected in these experiments. For the driving currents and the meaning of the remainder of the symbols, see Fig. 4.

electrolyte systems suggest that the calculated parameters enabled an optimum electrolyte system to be found from the considered alternatives (after the spacing constituents had been chosen). It is apparent that the choice of the spacing constituents can be optimized in an analogous way once the electrolyte system has been chosen.

TABLE II

OPERATIONAL SYSTEMS

BALA = β-Alanine; EACA = ε-aminocaproic acid; HEC = hydroxyethylcellulose; OAc^- = acetate.

Electrolyte	*Parameter*	*System No.*		
		1	*2*	*3*
Leading	Solvent	H_2O	H_2O	H_2O
	Anion	Cl^-	Cl^-	Cl^-
	Concentration (m*M*)	10	10	10
	Counter ion	BALA	BALA	EACA
	pH_L	3.2	4.0	4.7
	Additive	HEC	HEC	HEC
	Concentration (%, w/v)	0.2	0.2	0.2
Terminating	Solvent		H_2O	
	Anion		OAc^-	
	Concentration (m*M*)		5	
	Counter ion		H^+	
	pH_T		*ca.* 4.0	

TABLE III

CALCULATED AND EXPERIMENTALLY DETERMINED VALUES OF PARAMETERS CHARACTERIZING THE INFLUENCE OF MATRIX CONSTITUENTS ON THE QUANTIFICATION OF BENZOATE

Succinate, glutarate and acetate (terminating anion) served as spacing constituents.

Calculated data

2D system No.	*Sequence of the leading electrolytes*	$_1A$	$_2A$	$_{1-2}A$	ΔS_x
I	3.2/4.0	32.95	31.55	13.77	0.582
II	3.2/4.7	32.95	34.24	1.68	0.949
III	4.7/3.2	34.24	32.95	1.68	0.951
IV	4.0/4.7	31.55	34.24	1.91	0.939

Experimental data[a]

2D system No.	*Sequence of the leading electrolytes*	$_1A^*$	$_2A^*$	$_{1-2}A^*$	ΔS_x^*
I	3.2/4.0	395	1071	169	0.572
II	3.2/4.7	395	6705	78	0.803
III	4.7/3.2	6705	395	160	0.976
IV	4.0/4.7	1070	6705	373	0.651

[a] $_1A^*$, $_2A^*$ and $_{1-2}A^*$ values are given in thousands of counts of the integrator; the tabulated data are average values obtained from three determinations carried out with separately prepared electrolyte solutions from the same chemicals and from the same water purification system (relative standard deviations were 2–7%).

From the tabulated ΔS_x values it can be seen that also the predictions of the clean-up efficiencies of the 2nd separation steps based on the calculations were in reasonable agreement with the values based on experimental data (1.7–36% relative standard deviations). On the other hand, the ratios of $_1A$ and $_2A$ values for given combinations of the leading electrolytes deviate considerably from the corresponding ratios based on experimental data ($_1A^*$ and $_2A^*$ in Table III). These deviations suggest that the constituents representing the sample matrix in the experimental examination of the proposed procedure did not meet the assumption concerning the uniform distribution of the matrix constituents within an ionic mobility–pK "space" (see Theoretical). The ITP profiles in Fig. 4 also support this suggestion. These results indicate that theoretical models considering more appropriate distribution functions[5] for the ionic mobilities and/or pK values could lead to better agreements between the calculated and experimental data. However, we feel that the choice of the distribution function(s) should be closely related to the nature of the sample matrix. In practical situations a small number of preliminary experiments can be helpful in finding the most appropriate distribution function(s).

Despite the above discrepancies, it is apparent that the proposed procedure based on a very simple model can be helpful in minimizing the number of experiments necessary to find optimum working conditions in 2D ITP trace analysis of constituents detectable by selective detectors with quantification by the spike method. Its

application to the solution of practical analytical problems and its further refinement are subjects of our current research.

REFERENCES

1 F. M. Everaerts, Th. P. E. M. Verheggen and F. E. P. Mikkers, *J. Chromatogr.*, 169 (1979) 21.
2 J. C. Reijenga, A. A. G. Lemmens, Th. P. E. M. Verheggen and F. M. Everaerts, *J. Chromatogr.*, 320 (1985) 67.
3 F. E. P. Mikkers, F. M. Everaerts and J. A. F. Peek, *J. Chromatogr.*, 168 (1979) 293.
4 J. C. Giddings, *J. High Resolut. Chromatogr. Chromatogr. Commun.*, 10 (1987) 319.
5 E. Kenndler, *Anal. Chim. Acta*, 173 (1985) 139.
6 P. Boček, M. Deml and J. Janák, *J. Chromatogr.*, 156 (1978) 323.
7 L. Arlinger, *J. Chromatogr.*, 91 (1974) 785.
8 M. Svoboda and J. Vacík, *J. Chromatogr.*, 119 (1976) 539.
9 D. Kaniansky, V. Madajová, J. Marák, E. Šimuničová, I. Zelenský and V. Zelenská, *J. Chromatogr.*, 390 (1987) 51.
10 J. P. M. Wielders and F. M. Everaerts, in B. J. Radola and D. Graesslin (Editors), *Electrofocusing and Isotachophoresis*, Walter de Gruyter, Berlin, 1977, p. 527.
11 J. Marák, D. Kaniansky and V. Madajová, *Acta Fac. Rerum Nat. Univ. Comenianae Chim.*, 36 (1988) 91.
12 T. Hirokawa and Y. Kiso, *J. Chromatogr.*, 257 (1983) 197.
13 T. Hirokawa, H. Takemi, Y. Kiso, R. Takiyama, M. Morio, K. Fujii and H. Kikuchi, *J. Chromatogr.*, 305 (1984) 429.
14 T. Hirokawa, T. Tsuyoshi and Y. Kiso, *J. Chromatogr.*, 408 (1987) 27.
15 F. M. Everaerts, J. L. Beckers and Th. P. E. M. Verheggen, *Isotachophoresis—Theory, Instrumentation and Applications*, Elsevier, Amsterdam, Oxford, New York, 1976.
16 J. L. Beckers, *Thesis*, University of Technology, Eindhoven, 1973.
17 D. Kaniansky, V. Madajová, M. Hutta and I. Žilková, *J. Chromatogr.*, 286 (1984) 395.
18 F. E. P. Mikkers, S. Ringoir and R. de Smet, *J. Chromatogr.*, 162 (1979) 341.
19 M. Hutta, E. Šimuničová, D. Kaniansky, J. Tkáčová and J. Brtko, *J. Chromatogr.*, 470 (1989) 223.
20 D. Kaniansky, *Thesis*, Komenský University, Bratislava, 1981.
21 K. Rektorys, *Přehled Užité Matematiky*, SNTL, Prague, 4th ed., 1981, p. 397.
22 D. D. Perrin, W. L. F. Armarego and D. R. Perrin, *Purification of Laboratory Chemicals*, Pergamon Press, Oxford, 2nd ed., 1980.
23 T. Hirokawa, M. Nishino, N. Aoki, Y. Kiso, Y. Sawamoto, T. Yagi and J. I. Akiyama, *J. Chromatogr.*, 271 (1983) D1.